RoCoF-Constrained Scheduling Incorporating Non-Synchronous Residential Demand Response

Pádraig Daly, Hassan W. Qazi, and Damian Flynn, *Senior Member, IEEE*

***Abstract*—Demand response has the potential to provide a multitude of operating reserve categories. However, if integrated at scale, the non-synchronous nature of most demand response sources must be recognised within the operational rules of low inertia power systems. Here, a candidate non-synchronous reserve resource is considered within the scheduling and frequency stability time frames. It is shown that a detrimental impact on the post-contingency rate of change of frequency (RoCoF) can arise, potentially requiring the development of system operator policies to ensure that security standards are not compromised, as the volume of reserve available from non-synchronous reserve resources increases. A commitment-and-dispatch RoCoF constraint within scheduling procedures is proposed, which is independently verified using time domain simulations.**

***Index Terms*—non-synchronous resources, rate of change of frequency (RoCoF), synchronous inertia, unit commitment.**

NOMENCLATURE

A. Sets and Indices

$\mathcal{A}$	Set of dwelling archetypes, indexed by a.
$\mathcal{E}$	Set of hot water end uses, indexed by e.
$\mathcal{G}$	Set of generation resources, indexed by g.
$\mathcal{G}^{ns}$	Set of non-synchronous resources ($\subset \mathcal{G}$).
$\mathcal{G}^{stor}$	Set of storage resources.
$\mathcal{H}$	Set of electric water heater appliances, indexed by h.
$\mathcal{I}$	Set of time domain simulation time steps, indexed by i.
$\mathcal{K}$	Set of days, indexed by k.
$\mathcal{L}$	Set of high voltage direct current interconnectors between asynchronous ac systems, indexed by l.
$\mathcal{OR}$	Set of operating reserve categories, indexed by or.
$\mathcal{OR}^{con}$	Set of contingency reserve categories.
$\mathcal{OR}^{flex}$	Set of flexibility reserve categories.
$\mathcal{RS}$	Set of operating reserve resources, indexed by rs.
$\mathcal{RS}^{dyn}$	Set of dynamic reserve resources.
$\mathcal{T}$	Set of unit commitment and economic dispatch time periods, indexed by t.
$\mathcal{X}$	Set of candidate contingency events (large generators and high voltage direct current interconnectors), indexed by x.
$\mathcal{Z}$	Set of hot water draw events, indexed by z.

B. Parameters

A_h^{tk}	Tank surface area, appliance h (m^2).
C_g^{nl}	No load cost, resource g (€/h).
$DB^{uf/of}$	Fleet response deadband for an under/over-frequency event (Hz).
$\overline{P}_h$	Rated power draw, appliance h (MW).
$\overline{P}_h^{loss}$	Rate of heat loss, appliance h (MW).
$\overline{P}_h^{supply}$	Rate of heat supplied, appliance h (MW).
$\underline{E}$	Synchronous stored rotational energy (inertia) lower limit (MWs).
EFF_h	Efficiency, appliance h.
F^{nom}	Nominal frequency (Hz).
H_g	Inertia constant, resource g (s).
$M_h^{wr,tk}$	Tank water mass, appliance h (kg).
N^{rocof}	Number of time domain simulation steps within the rate of change of frequency calculation window.
$\underline{P}_g$	Minimum power output, resource g (MW).
$\overline{P}_g$	Maximum power output, resource g (MW).
$P_{l,t}^{imp/exp}$	Power import/export, link l, period t (MW).
P_t^{load}	Demand (excluding storage charging), period t (MW).
$\overline{R}_{EWH,or,t}$	Maximum reserve capability from the electric water heater fleet, category or, period t (MW).
$\overline{R}_{rs,or,t}$	Maximum reserve capability, resource rs, category or, period t (MW).
$\underline{REQ}_{or,t}$	Requirement, category or, period t (MW).
RF_{or}	Requirement factor, category or.
$\lvert\overline{ROCOF}\rvert$	Rate of change of frequency magnitude upper limit (Hz/s).
$RR^{uf/of}$	Fleet response range for an under/over-frequency event (Hz).
$\overline{S}_g$	Apparent power rating, resource g (MVA).
$\overline{SNSP}$	Non-synchronous penetration upper limit.
$T_{e,z,k}^{draw}$	Hot water draw duration, end use e, event z, day k (s).
T^{per}	Time period duration (h).
T^{rocof}	Rate of change of frequency calculation window (s).
T^{step}	Time step size (s).
U_h^{tk}	Tank U-value, appliance h (MW/m^2°C).
V_e	Volumetric flow rate, end use e (m^3/s).
$VOLL$	Value of lost load (€/MWh).

The work of P. Daly was supported by the Irish Research Council's Embark Initiative. The work of H. W. Qazi was supported by Science Foundation Ireland under grant number 09/IN.1/I2608.

D. Flynn is with the School of Electrical and Electronic Engineering, University College Dublin, Ireland, (e-mail: damian.flynn@ucd.ie).

P. Daly and H. W. Qazi are currently working in industry (e-mail: padraig.daly@ucdconnect.ie; hassanwqazi@gmail.com).

$VORS_{or}$	Value of reserve shortage, category or (€/MW).
W^c	Water specific heat capacity (MJ/kg°C).
W^ρ	Water density (kg/m^3).
Γ_{or}	Fleet proportion capable of providing reserve, category or.
Θ^{air}	Ambient air temperature (°C).
$\Theta^{wr,in}$	Inlet water temperature (°C).
$\Theta_h^{wr,tk}$	Tank water temperature, appliance h (°C).
$\underline{\Theta}_h^{wr,tk}$	Tank water lower setpoint, appliance h (°C).
$\overline{\Theta}_h^{wr,tk}$	Tank water upper setpoint, appliance h (°C).
Λ_h	On/off status, appliance h.
$\Lambda_{h,t}$	On/off status, appliance h, period t.
Ω_h	Frequency response threshold, appliance h (Hz).
Ψ	Frequency response hysteresis (Hz).

C. Variables

$c_{g,t}^p$	Production cost, resource g, period t (€/h).
$c_{rs,or,t}^r$	Reserve cost, resource rs, category or, period t (€).
$c_{g,t}^{su}$	Start-up cost, resource g, period t (€).
$f_{x,i}$	Frequency, event x, step i (Hz).
f_i	Frequency, step i (Hz).
$snsp_t$	Non-synchronous penetration, period t.
$p_{g,t}$	Power output, resource g, period t (MW).
$p_{g,t}^{load}$	Charging demand, resource g, period t (MW).
$p_{x,t}$	Power output/flow, candidate event x, period t (MW).
$r_{g,or,t}$	Reserve provision, resource g, category or, period t (MW).
$r_{rs,or,t}$	Reserve provision, resource rs, category or, period t (MW).
$u_{g,t}$	Commitment status, resource g, period t.
$v_{g,t}$	Start-up status, resource g, period t.
$w_{g,t}$	Time since shut-down, resource g, period t (h).
$rocof_{x,i}$	Rate of change of frequency, event x, step i (Hz/s).
$\lvert rocof^{max}\rvert$	Maximum rate of change of frequency magnitude (Hz/s).
Δf_i	Frequency deviation, step i (Hz).
$\lambda_{h,i}^{uf}$	Frequency control signal, appliance h, step i.
$\nu_{a,k}$	Hot water consumption, archetype a, day k (m^3).
ϕ_t^p	Load not served, period t (MW).
$\phi_{or,t}^r$	Reserve not served, category or, period t (MW).

I. Introduction

AS POWER systems integrate higher shares of low marginal cost, non-synchronous generation, the number of conventional units online reduces. Such a decline in the traditional providers of frequency control establishes a need to incentivise investments in new resources and/or upgrades to existing resources, so that sufficient frequency control capability is available during periods of high non-synchronous penetrations—periods of potential ancillary/system service scarcity, otherwise.

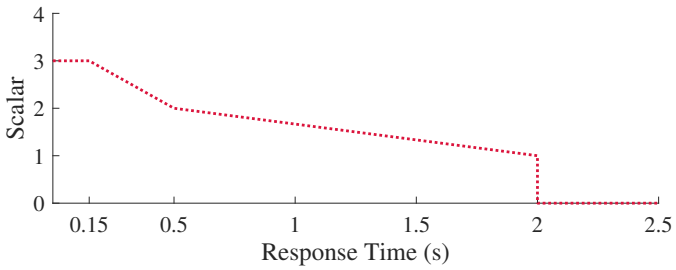

Fig. 1. Payment scalar for faster deployment speeds of fast frequency response, Ireland and Northern Ireland [4]

In power systems with low stored rotational energy (inertia), fast-acting frequency control is paramount: lower online inertia levels can manifest as a reduction in the time to reach the maximum frequency deviation, which may be too fast for full primary frequency response deployment [1]. AEMO, amongst a number of system operators, is exploring the capability of non-synchronous technologies to provide fast-acting frequency control [2]. National Grid has designed a system service that recognises the value of a speed of response faster than primary frequency control [3]. EirGrid and SONI are introducing a payment scalar in order to incentivise a fast frequency response that is faster than the 'base-line' design (2 s) [4]. As shown in Fig. 1, a threefold payment rate can be attained for a response time less than or equal to 0.15 s. With such developments, non-traditional frequency control providers, e.g. variable speed wind turbines, solar photovoltaics, converter-interfaced energy storage and demand response (DR)—which heretofore may have viewed the ancillary-service-provision return on investment as unfavourable—are beginning to provide frequency control services, amongst others, in greater volumes.

A non-synchronous reserve resource can affect the operation of the power system over multiple time frames, with the impact in one time frame potentially having consequences in another. For example, in the scheduling time frame, reserve provision from non-synchronous resources can result in higher outputs for some generators that were previously part-loaded for reserve (headroom) purposes, potentially leading to an increase in the active power imbalance following a loss of generation event. Reserve provision from non-synchronous resources can also result in the displacement of some higher marginal cost synchronous units, leading to a reduction in online inertia. With lower online inertia and higher unit outputs, the likelihood of higher post-contingency rate of change of frequency (RoCoF) magnitudes, in the short-term frequency stability time frame, may increase [5]. High RoCoF magnitudes can lead to operational security issues, which may offset some of the benefits of non-synchronous reserve. These include the tripping of gas turbines due to lean blow out [6], the tripping of synchronous generation due to reverse power flow [7], and/or the cascade tripping of RoCoF-based anti-islanding relays for distributed generation [8]. Further, if protection activation results in a higher generation-load imbalance, the accompanying frequency deviation can result

in turbine blade damage of thermal units [9], the oscillatory behaviour of dual-input power system stabilisers [10], and/or pole slipping of machines while operating at leading power factor, subsequently resulting in a generation trip [11].

Thus, although the potential economic benefits of demand-side reserve provision have been shown [12], the impact of such reserve provision on the inertial response of systems with high shares of non-synchronous energy resources, such as variable speed wind turbines and solar photovoltaics, must also be determined.

Many non-synchronous technologies have been considered within the unit commitment and economic dispatch (UCED) time frame. For example, how high voltage direct current (HVDC) interconnection can aid the frequency stability of asynchronously interconnected systems, by sharing primary operating reserves across the connected systems and utilising HVDC emergency control is shown in [13]; while the potential benefits of the frequency control capability of battery energy storage are demonstrated in [14]. Of course, all such technologies are likely to require a market framework to incentivise reliable responses [15].

Alongside these approaches, constraints within UCED relating to the post-contingency frequency nadir [16], [17] and quasi-steady-state deviation [16], [18] have been proposed. However, as the share of non-synchronous resources increases, greater attention on the time frame preceding the nadir and the quasi-steady-state deviation, i.e. the inertial time frame, is required. Consequently, RoCoF is a metric of emerging importance.

With respect to RoCoF constraints within UCED, proposals to date can be categorised into two forms. Firstly, a *commitment-only* ('inertia floor') RoCoF constraint [14], [16], which sets a minimum system inertia requirement fixed for all time periods across the simulation, by employing a predetermined worst-case event (typically based on the maximum output of the largest generator). Such a formulation can often lead to inefficient surpluses of synchronous inertia being carried at times when the worst-case RoCoF event online does not equal that used in the design of the inertia floor. Secondly, a *dispatch-only* RoCoF constraint [13], [19], which dispatches down the binding contingency so that the RoCoF limit is not exceeded. Such a formulation is most efficient within real-time security-constrained economic dispatch, as on/off commitment decisions are not possible.

The main contributions of this paper are as follows:

1) The RoCoF implications of integrating a non-synchronous reserve resource are demonstrated. In order to redress the resulting degradation in system RoCoF, an integrated *commitment-and-dispatch* RoCoF constraint is presented. Such a formulation improves the operational efficiency of a RoCoF requirement within UCED, by allowing the system synchronous inertia level to dynamically vary with changes in the output of N$-$1 events online, which, for some systems, can vary over a wide range across a day, week, or outage season.
2) By conducting UCED and distinct time domain simulations for a full year of operation, both system scheduling criteria, such as production cost and carbon dioxide (CO_2) emission, and short-term frequency stability criteria, such as RoCoF and nadir, are presented within a modelling framework, demonstrating how a system operator might evaluate and address the RoCoF impacts of non-synchronous reserve resources.

Section II outlines the models and test system used. Section III demonstrates the RoCoF implications of scheduling and deploying non-synchronous reserve resources. Section IV presents an evaluation of the system impact of non-synchronous reserve resources, and Section V concludes.

II. Methodology

A. Modelling Framework

In order to investigate the operational impact of a non-synchronous resource, two time frames are modelled: the UCED time frame, using an hourly resolution, and separately the short-term frequency stability time frame, using a 10 ms resolution. Modelling the impact of a non-synchronous resource on the UCED schedule is critical to revealing the short-term frequency stability impacts: UCED determines the pre-contingency system operating point and the size of the largest online event, both of which have a significant bearing on the post-contingency system dynamic behaviour. Thus, two representations of a candidate non-synchronous reserve, residential electric water heating (EWH), are included: (i) for the UCED model (reserve scheduling), and (ii) for the short-term frequency stability model (reserve deployment).

The modelling framework employed is summarised in Fig. 2, which shows the data flow between the time frames. Note that the UCED model and the stability model are simulated separately: following completion of a full UCED simulation there is a unidirectional flow of data to the stability model, i.e. there is no explicit feedback/iterative process in the framework. The stability model is an independent module in the framework, allowing for security constraint additions in UCED to be validated, by simulating the resulting system short-term frequency stability behaviour. Each UCED simulation is conducted for a year of operation, which yields a multitude of system operating points, e.g. changing patterns of HVDC IC flows and generator dispatch decisions, which together define the worst-case event online (and hence the contingency reserve requirement), and the generator commitment decisions, which define the system inertia level. These time periods are then used to initialise thousands of distinct time domain simulations.

The test system used is detailed in Section II-B. The UCED model is described in Section II-C. The EWH reserve availability model, which is an input to the UCED model, is given in Section II-D. The short-term frequency stability model is described in Section II-E. The frequency control scheme employed for EWH, which is an integral part of the stability model, is given in Section II-F. The simulation cases and scenarios are outlined in Section II-G.

B. Test System

The Ireland and Northern Ireland system, a single synchronous (island) power system, spanning the jurisdictions of

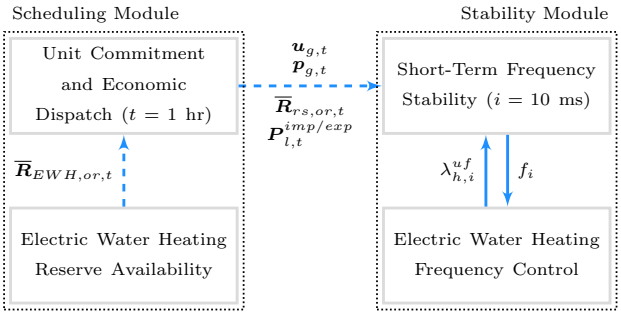

Fig. 2. Modelling framework. A dashed line indicates data flow between models solved separately. Bold typeface indicates time series data (year-long at an hourly resolution)

Ireland and Northern Ireland, is the test system considered. The system is characterised by high levels of wind power, which is approximately evenly split between the transmission and distribution systems. The conventional portfolio is predominantly gas-fired, the majority of which are combined cycle gas turbines (CCGTs) and open cycle gas turbines (OCGTs). The remaining conventional fleet is comprised of thermal units, some of which are also fired by gas, as well as coal, oil, and indigenous peat. There are also distillate-fired combustion turbines, run-of-the-river hydro and a pumped hydroelectric storage (PHS) plant. There is 1 GW of HVDC interconnection with Great Britain: a 500-MW line-commutated converter HVDC IC that links Northern Ireland and Scotland, and a 500-MW voltage-source converter HVDC IC that links Ireland and Wales. Peak demand (winter day) for the study is taken as 7.1 GW, and minimum demand (summer night) is taken as 2.4 GW, with an annual total energy requirement of 39.3 TWh. A summary of the modelled energy portfolio is given in Table I. Perfect foresight of wind power is assumed.

The UCED plant data are taken from [20], the fuel prices from [21], with an aggregated (by fuel type) model of the Great Britain system used [22]. Forced and scheduled outages, from historical experience, are included. Conventional unit must-run constraints for voltage control and reactive power support in particular network locations are included [23]. It is forecasted, and assumed here, that such constraints will be reduced due to planned network development in future years. A schematic of Ireland and Northern Ireland power system can be found in [24].

C. Unit Commitment and Economic Dispatch Model

The expected system operational cost is minimised using PLEXOS [25] and the Xpress-MP mixed integer programming solver [26]. The objective function is given in (1).

$$\min \sum_{t\in\mathcal{T}} \Bigg\{ T^{per}\cdot\phi^{p}_{t}\cdot VOLL + \sum_{or\in\mathcal{OR}} \phi^{r}_{or,t}\cdot VORS_{or} + \sum_{g\in\mathcal{G}} \Big\{ c^{su}_{g,t}(v_{g,t},w_{g,t}) + T^{per}\cdot\big[u_{g,t}\cdot C^{nl}_{g} + c^{p}_{g,t}(p_{g,t})\big] \Big\} + \sum_{or\in\mathcal{OR}}\sum_{rs\in\mathcal{RS}} c^{r}_{rs,or,t}(r_{rs,or,t}) \Bigg\} \quad (1)$$

TABLE I
TEST SYSTEM ENERGY PORTFOLIO

Technology	**Capacity (MW)**
Wind power	4,250/6,000 (current/future)
HVDC interconnection	1,000
Fossil thermal (coal, gas, peat, oil)	2,439
Combined cycle gas turbine	4,208
Hydro (incl. pumped storage)	504
Open cycle gas turbine	655
Distillate combustion turbine	631
Combined heat and power	238

where the horizon, $\mathcal{T}$, consists of time periods, t, of duration T^{per} (one hour). Each generation resource, g, in the set $\mathcal{G}$, can have a start-up cost function, c^{su} (hot, warm and cold starts are modelled, determined by the number of time periods since shut down, w, and the start-up status, v), a no-load cost, C^{nl} (multiplied by the commitment status, u), and a production cost function, c^{p} (depending on the active power output, p). Each reserve resource, rs, in the set $\mathcal{RS}$, can have a reserve cost, c^{r}, dependent on its provision, r.

Unserved load, ϕ^{p}, and reserve, ϕ^{r}, are respectively penalised at the value of lost load, $VOLL$, and the value of reserve shortage, $VORS$.

The set of operating reserve categories modelled, $\mathcal{OR}$, indexed by or, based on [23], is comprised of subsets of contingency reserves (frequency response for large disturbance events), $\mathcal{OR}^{con}$, and flexibility reserves (ramping margin for net load variability/uncertainty), $\mathcal{OR}^{flex}$. Both $\mathcal{OR}^{con}$ and $\mathcal{OR}^{flex}$ are comprised of upward, U, and downward, D, subsets. The contingency reserves include primary, POR, secondary, SOR, tertiary-I, and $TOR1$, tertiary-II, $TOR2$, while a flexibility reserve is denoted by $FLEX$. As the delivery times do not overlap, a resource can simultaneously provide all categories of upward contingency reserve. A summary of these reserves, including the parameters which set the requirements, is given in Table II.

The contingency reserve constraints are given by (2).

$$\sum_{rs\in\mathcal{RS}}^{rs\neq x} r_{rs,or,t} \geq p_{x,t}\cdot RF_{or}, \quad \forall x\in\mathcal{X}, or\in\mathcal{OR}^{con}, t \quad (2)$$

where x is the index of the set of contingency events, $\mathcal{X}$. For the upward contingency reserve categories this includes in-service infeeds, i.e. large online generators and importing HVDC ICs. For the downward contingency reserve category this includes in-service outfeeds, i.e. exporting HVDC ICs and online loads. RF is the requirement factor, which determines what fraction of the binding event must be carried as reserve, for a given category, see Table II. Given the existence of staggered generation shedding schemes and wind power turn-down (droop) capability for over-frequency events, a lower requirement factor is specified for downward contingency reserve in comparison to those for upward contingency reserve, see Table II.

'Static'[1], i.e. step-like, non-frequency-tracking once trig-

[1]For further detail on static and dynamic response types, refer to [27].

TABLE II
OPERATING RESERVES

Category	Time to Full Deployment	RF_{or} (fraction of binding event)	$\underline{REQ}_{or,t}$ (MW) Day	Night
POR^U	5 s	0.75	160	125
POR^D	5 s	0.50	100	100
SOR^U	15 s	0.75	–	–
$TOR1^U$	90 s	1.00	–	–
$TOR2^U$	5 min.	1.00	–	–
$FLEX^U$	1 hr	–	150	150
$FLEX^D$	1 hr	–	150	150

gered, responses (at discrete frequency thresholds), e.g. from PHS when pumping, can provide upward contingency reserve. However, minimum 'dynamic', i.e. governor-like, response requirements are enforced for primary operating reserves, (3).

$$\sum_{rs \in \mathcal{RS}^{dyn}} r_{rs,POR^U,t} \geq \underline{REQ}_{POR^U,t} \quad \forall t \tag{3}$$

where $\mathcal{RS}^{dyn}$ is the dynamic reserve resource set, and $\underline{REQ}$ is the requirement. Equation (3) is shown for upward primary operating reserve, POR^U. A similar constraint is enforced for downward primary operating reserve, POR^D. As well as during export periods, the dynamic response requirement for POR^D applies during import periods in order to cater for loss of load events.

The constraint for upward flexibility reserve, $FLEX^U$, sourced from conventional units only, is given in (4).

$$\sum_{g \notin \mathcal{G}^{ns}} r_{g,FLEX^U,t} \geq \underline{REQ}_{FLEX^U,t} \quad \forall t \tag{4}$$

where $\mathcal{G}^{ns}$ is the set of non-synchronous generators. A similar constraint is enforced for $FLEX^D$.

Equations (5)–(7) introduce additional constraints relating to upward and downward reserve provision from resources.

$$p_{g,t} + r_{g,or,t} + r_{g,FLEX^U,t} \leq u_{g,t} \cdot \overline{P}_g \quad \forall g, or \in \mathcal{OR}^{conU}, t \tag{5}$$

$$p_{g,t} - r_{g,POR^D,t} - r_{g,FLEX^D,t} \geq u_{g,t} \cdot \underline{P}_g \quad \forall g, t \tag{6}$$

$$r_{rs,or,t} \leq \overline{R}_{rs,or,t} \quad \forall rs, or, t \tag{7}$$

where $\underline{P}$ is the minimum power output, $\overline{P}$ is the maximum output, $\overline{R}$ is the maximum reserve capability, and $\mathcal{OR}^{conU}$ is the upward contingency reserve subset.

In order to assess the stability implications for a future Ireland and Northern Ireland power system with high shares of renewable energy sources (RES), a suite of analyses, termed the *Facilitation of Renewables* studies, was carried out [28]. Based on these stability studies, an operational security metric, the system non-synchronous penetration (SNSP), was devised and applied in real-time. In order to ensure that an appropriate operational bound is enforced for the SNSP within UCED, an upper limit, $\overline{SNSP}$, is applied (8a). SNSP is the quotient of the power from non-synchronous infeeds and the total demand, (8b).

$$snsp_t \leq \overline{SNSP} \quad \forall t \tag{8a}$$

where

$$snsp_t = \frac{\sum_{g \in \mathcal{G}^{ns}} p_{g,t} + \sum_{l \in \mathcal{L}} P^{imp}_{l,t}}{P^{load}_t + \sum_{g \in \mathcal{G}^{stor}} p^{load}_{g,t} + \sum_{l \in \mathcal{L}} P^{exp}_{l,t}} \tag{8b}$$

where $snsp$ is the non-synchronous penetration for a given time period, and $\mathcal{G}^{ns}$ is the non-synchronous generator set, which includes non-synchronous storage, e.g. batteries. The set $\mathcal{L}$, indexed by l, consists of HVDC ICs connecting the synchronous system under study to adjacent but asynchronously interconnected systems. HVDC IC flows, $P^{imp/exp}$, are fixed inputs from an 'unconstrained' (market) simulation, with superscripts imp/exp denoting an import/export to/from the synchronous system. Demand is denoted by the superscript $load$, and is made up of price-inelastic demand, P^{load}, and storage charging, p^{load}, with $\mathcal{G}^{stor}$ denoting the storage set. A variable for demand-side participation in the energy market could be included within the denominator of (8).

The exact upper limit for the permissible penetration of non-synchronous infeeds is system specific and requires detailed stability analysis across a wide range of future operational scenarios. The limit is a complex function of network size, generation and demand mix, grid code standards, and the system service framework in place to stipulate/incentivise technical performance (during contingencies). The limit itself will change over time as measures are introduced [29].

D. Demand Response for Contingency Reserve Provision

Many loads can provide operating reserve: potential sources include water heating, space heating, cooling and ventilation, lighting, refrigeration, and motor load (including compressors, fans, pumps), across the residential, commercial, municipal, industrial and agricultural sectors [30].

From an inertial response perspective, such loads can be segregated into rotating and non-rotating loads. However, with the tripping of a load resulting in its accessible inertial contribution (if any) no longer being online, demand-side reserve provision, following activation, is non-synchronous.

The extent of a load's contingency reserve potential is determined by criteria such as share of electricity consumption, and end user patterns and constraints. For example, electric space heating, although possessing a significant thermal storage capacity, has low through-the-year availability (albeit climate dependent); refrigeration, although exhibiting consistent availability, is generally a small component of electricity consumption. Residential electric water heating (EWH), due to its sizeable thermal storage capacity, year-round availability and large share of residential demand, is a suitable candidate for contingency reserve provision [31], and hence is taken as the representative non-synchronous resource.

In order to ensure appliance heterogeneity (with regard to water tank capacity and daily hot water consumption), four dwelling types, which characterise the Ireland housing stock, are modelled: detached, terraced, semi-detached and

apartment. The hot water consumption volume, ν, per dwelling type, a, on a given day, k, is given in (9).

$$\nu_{a,k} = \sum_{z \in \mathcal{Z}} \sum_{e \in \mathcal{E}} T^{draw}_{e,z,k} \cdot V_e, \quad \forall a, k \tag{9}$$

where T^{draw} is the duration of a given hot water draw event, z, for a given end use, e, on a given day. Each end use (shower, bath, hand wash, dish wash) has a given volumetric flow rate, V. The occurrence of a water draw event is determined probabilistically, according to day, week and season, based on surveyed data [32].

In order to accurately capture the impact of individual load states, as well as temporal variability, a bottom up characterisation of EWH is used, i.e. classical single node models, based on the energy balance within a water tank, considering both heat exchange with the surroundings and hot water draw events. Assuming that the inlet and outlet water flow rates are equal, the rate of change of the tank water temperature, for an appliance, h, in the water heater population, $\mathcal{H}$, is given by (10a).

$$\frac{d\Theta^{wr,tk}_h}{dt} = \frac{1}{M^{wr,tk}_h \cdot W^c} \left[\Lambda_h \cdot P^{supply}_h - P^{loss}_h \right] \tag{10a}$$

where

$$P^{supply}_h = EFF_h \cdot \overline{P}_h \tag{10b}$$

and

$$\begin{aligned} P^{loss}_h = {} & U^{tk}_h \cdot A^{tk}_h \cdot \left[\Theta^{wr,tk}_h - \Theta^{air} \right] \\ & + W^{\rho} \cdot V_e \cdot W^c \left[\Theta^{wr,tk}_h - \Theta^{wr,in} \right] \end{aligned} \tag{10c}$$

where the rate of heat supply, P^{supply}, is determined by the rated power draw, $\overline{P}$, and efficiency EFF of the heating element, (10b). The rate of heat loss, P^{loss}, has two components: (i) the heat exchange with the surroundings (at ambient temperature, Θ^{air}), which is determined by the tank U-value, U^{tk}, and surface area, A^{tk}, and (ii) in the event of a water draw event, the heat exchange with the cold inlet water (at $\Theta^{wr,in}$), which is determined by the end use volumetric flow rate as well as the specific heat capacity, W^c, and density, W^{ρ}, of water, (10c). A constant tank water mass, $M^{wr,tk}$, is assumed.

The on/off status, Λ, is determined by thermostat control, which regulates the tank water temperature, $\Theta^{wr,tk}$, between lower, $\underline{\Theta}^{wr,tk}$, and upper, $\overline{\Theta}^{wr,tk}$, setpoints.

Combining dwelling-type water consumption patterns, (9) and appliance thermal models, (10), distinct EWH models are developed in order to capture the stochastic nature of an EWH population ($\sim$10% of households in the test system).

The point of predictable stochasticity for aggregate load profile varies with the level of detail included in the individual load models and parameter variation [33], [34]. In order to determine the point of predictable stochasticity, the number of individually modelled loads was increased until the aggregate profile obtained a consistent pattern, unchanged by an increase in the number of individual loads. This number was found to be $\sim$2,000 water heaters.

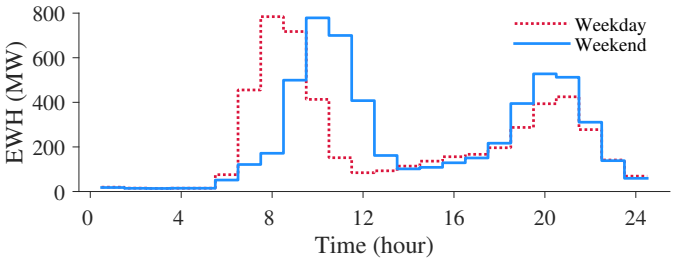

Fig. 3. Mean (across a year) EWH upward contingency reserve availability

Aggregating the EWH models yields an estimation of the reserve available from the EWH population, EWH, for upward and downward contingency reserves, as given by (11) and (12), respectively.

$$\overline{R}_{EWH,or,t} = \sum_{h \in \mathcal{H}} \Lambda_{h,t} \cdot P^{supply}_h \cdot \Gamma_{or} \quad \forall or \in \mathcal{OR}^{conU}, t \tag{11}$$

$$\overline{R}_{EWH,POR^D,t} = \sum_{h \in \mathcal{H}} P^{supply}_h \left[1 - \Lambda_{h,t} \right] \cdot \Gamma_{POR^D} \quad \forall t \tag{12}$$

where Γ denotes the proportion of the EWH fleet that can provide a given operating reserve category. Due to the significant thermal storage capacity of EWH, it is assumed that equal availability ($\Gamma_{or} = 1$) is offered from the primary to tertiary-II time frames. If a flexible load cannot be switched off for a sufficient duration, demand-side reserve provision is unlikely to significantly reduce the number of synchronous generators online, as it will be necessary to keep units online to meet longer duration contingency reserve requirements.

Fig. 3 presents the mean hourly upward contingency reserve available from EWH. Although small summer-winter differences exist, inter-hourly variability dominates. Fig. 3 demonstrates the considerable reserve available from EWH. However, between midnight and 6 a.m. EWH availability is at its lowest, implying generators (or other means) must be employed to meet the reserve requirements. If other flexible loads were harnessed, the valleys present in the double-humped EWH availability profile could be filled, e.g. time-of-use pricing could incentivise storage heating or electric vehicles to switch on/off at appropriate times. For simplicity of presentation, such an approach is not adopted here.

In order to capture worst-case conditions from a non-synchronous share perspective, it is assumed that EWH reserve offer prices are near zero: if the costs associated with scheduling a non-synchronous reserve resource were (onerously) high, its share would likely be low and thus its non-synchronous nature would not be of concern.

E. Short-Term Frequency Stability Model

A single busbar dynamic model of the Ireland and Northern Ireland system [28] has been developed in MATLAB and Simulink [35]. The model, verified against actual traces of the overall frequency response, is used for simulating the

frequency response of the system over the first 30 seconds following a contingency. The system frequency, calculated via integration of the active power imbalance, is used as an input to frequency sensitive load and generator models. Generator models include thermal [36], OCGT and CCGT [37], hydro [38], and variable speed wind turbine [39] models. No frequency control (emulated inertia or contingency reserve provision) is enabled from wind power, in order to isolate the impact of the EWH appliances (see Section II-G regarding emulated inertial control and the system RoCoF requirement). Both DR (EWH appliances) and non-DR loads are represented. The inherent frequency sensitivity of load is included in the non-DR component [40].

The inertia of units online are combined to form a system inertial term, which determines the initial post-contingency RoCoF. The increased use of variable frequency drives in induction motors, and in compressors for refrigeration and heating, ventilation, air conditioning appliances is resulting in the erosion of the inertial contribution from (modern) rotating loads. Hence, no load inertial contribution is assumed here, as a worst-case scenario.

For a given time period of the UCED schedule, the maximum system RoCoF magnitude from the time domain simulation, $|rocof^{max}|$, is calculated per (13).

$$|rocof^{max}| = \max\left\{|rocof_{x,i}|\right\}, \quad \forall x, i > N^{rocof} \tag{13a}$$

where

$$rocof_{x,i} = \frac{f_{x,i} - f_{x,i-N^{rocof}}}{T^{rocof}}, \quad \forall x, i > N^{rocof} \tag{13b}$$

$$N^{rocof} = \frac{T^{rocof}}{T^{step}} \tag{13c}$$

where f and $rocof$ denote frequency and RoCoF, respectively, and i is the integration time step of the time domain simulation. The time window over which RoCoF is calculated (500 ms) is denoted by T^{rocof}. A window of 500 ms corresponds to that chosen for the proposed RoCoF definition for the grid code [41], as well as that used by anti-islanding relays for distribution-connected generation, in Ireland. The (fixed) time domain simulation step size (10 ms) is denoted by T^{step}, and N^{rocof} is the quotient of the RoCoF window and the integration step size.

F. Demand Response for Frequency Control

With the development of cost-effective autonomous frequency sensors and controllers [42], decentralised demand-side control becomes feasible. While the literature includes the use of frequency derivative-based control, e.g. [43], it is assumed here that frequency derivative-based control is unsuitable due to the difficulties associated with noise in RoCoF measurements. Instead, a pseudo-governor control, i.e. based off the frequency deviation, Δf, is employed. The control signal, λ, determining individual appliance on/off switching in response to an under-frequency, uf, event is given by (14).

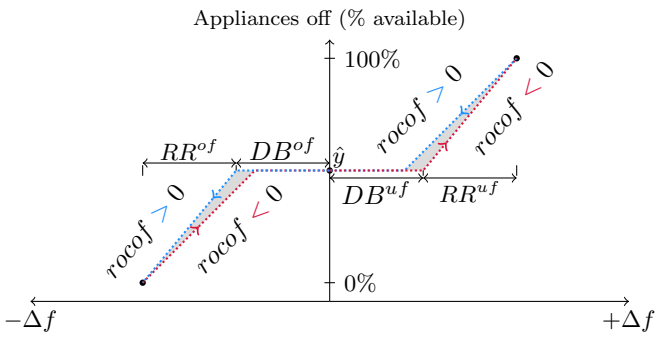

Fig. 4. Fleet pseudo-governor frequency control. (Not to scale of parameter values selected; the intersection point, $\hat{y}$, varies along the vertical axis, depending on the available volume)

$$\lambda^{uf}_{h,i} = \begin{cases} 0 & \text{if } \Delta f_i \geq \Omega_h \text{ or} \\ & \lambda^{uf}_{h,i-1} = 0 \text{ and } \Delta f_i \geq \Omega_h - \Psi \\ 1 & \text{otherwise} \end{cases} \tag{14a}$$

where

$$\Delta f_i = F^{nom} - f_i \tag{14b}$$

where Ω is the response threshold, Ψ is the control hysteresis, and F^{nom} is the nominal frequency. Over-frequency, of, control can be similar to that shown in (14).

The relationship between individual appliance control and the fleet pseudo-governor response is illustrated in Fig. 4. Beyond the aggregate response deadband (the smallest value of Ω in the fleet), $DB^{uf/of}$, the available flexible loads respond linearly to a frequency deviation across the response range (the largest value of Ω in the fleet), $RR^{uf/of}$. For example, for an under-frequency event, as the frequency falls, i.e. the RoCoF is negative, loads are tripped in a staggered manner. Following nadir formation, as the frequency rises towards steady-state, i.e. the RoCoF is positive, the loads are switched back on at a rate that differs (by Ψ) from their respective switch-off values, thus preventing oscillatory behaviour. Such fleet hysteresis, depicted by the shaded region in Fig. 4, helps mitigate loss of load diversity.

The employed values for the frequency control parameters are as follows. $DB^{uf} = 0.1$ Hz, which withholds response triggering for large disturbances; $RR^{uf} = 0.2$ Hz, which ensures an appropriate balance of response speed, to minimise frequency deviations, and robustness, to prevent oscillatory system frequency behaviour; $\Psi = 0.01$ Hz, which aids the return of the system frequency toward nominal; and a response time of 300 ms, which is within typical current controller limits [44], [45].

G. Test Cases and Scenarios

In order to explore the impact of a non-synchronous reserve resource on system scheduling and frequency stability, *cases* with and without EWH being available for contingency reserve provision and deployment, under current and future *scenarios* are considered.

The case without EWH being available is termed the 'synchronous reserve case' (sync-only case), while the case with EWH being available is termed the 'synchronous and non-synchronous reserve case' (sync+non-sync case). For each reserve case, two operational scenarios, current and future, are analysed in order to assess the impact of a non-synchronous reserve resource in different inertial contexts (the future operational scenario has further inertial reductions).

In order to fairly assess the reserve cases under the current and future operational scenarios, the EWH availability remains unchanged between them. Note that for clarity of (initial RoCoF) effect, EWH is the sole non-synchronous reserve resource considered; no frequency support is provided from non-synchronous energy resources, such as wind power (discussed further in Section IV-B).

The different assumptions taken for the current and future operational scenarios are shown in Table III. Between the current and future operational scenarios it is assumed that the installed wind power capacity and the SNSP limit increase, that the installation of dedicated network devices, e.g. static synchronous compensators, has allowed for a reduction in the number of regional synchronous generation must-run constraints for voltage control [23], and that the synchronous inertia floor is replaced by a commitment-and-dispatch RoCoF constraint due to the potential implications for RES curtailment with the former approach [5].

The inertia floor constraint (which assumes a nominal frequency), employed under the current operational scenario, is given by (15).

$$\sum_{g \notin \mathcal{G}^{ns}} u_{g,t} \cdot H_g \cdot \overline{S}_g \geq \underline{E} \quad \forall t \tag{15}$$

whereby the inertial contribution of a synchronous resource is the product of its inertia constant, H, apparent power rating, $\overline{S}$, and commitment status. Here, an inertia floor, $\underline{E}$, of 20 GWs is taken [23].

Equation (15) ensures that the system inertia remains above a constant minimum level. Such a value can be determined via offline stability analysis, by identifying the loss, X, that results in the highest RoCoF magnitude. In such a case, (15) becomes (16).

$$\sum_{gg \notin \mathcal{G}^{ns}}^{gg \neq g} u_{gg,t} \cdot H_{gg} \cdot \overline{S}_{gg} \geq \frac{F^{nom} \cdot \overline{P}_g}{2 \cdot \left|\overline{ROCOF}\right|} \quad \forall t, g = X \tag{16}$$

where $\left|\overline{ROCOF}\right|$ is the (operational) RoCoF magnitude limit that has been specified, and gg is an alias, which ensures that the inertia (if any) of the defining critical event (with maximum output $\overline{P}$), does not count toward the inertial total. Such a constraint is similar to that proposed in [14], [16]. The efficiency of (16) hinges on the number of time periods for which the defining critical event materialises as a potential contingency.

The RoCoF constraint employed under the future operational scenario is given by (17).

TABLE III
OPERATIONAL SCENARIOS

Parameter	Current	Future
Installed wind power (MW)	4,250	6,000
SNSP limit (%)	60	75
Min. units online, must-run for voltage control	6	3
RoCoF formulation	(15)	(17)

$$\sum_{s \in \mathcal{S}}^{s \neq x} u_{g,t} \cdot H_g \cdot \overline{S}_g \geq \frac{F^{nom} \cdot p_{x,t}}{2 \cdot \left|\overline{ROCOF}\right|}, \quad \forall x \in \mathcal{X}, t \tag{17}$$

Similar to a N−1 reserve constraint, (17) can be written for a subset of system resources, e.g. large generators and HVDC ICs, so as to ensure that the schedule is secure with respect to the single loss of any one of the resources considered as contingencies, for the specified RoCoF magnitude limit. If (17) is having a binding impact on the schedule for a given time period, the optimisation can either increase the system synchronous inertia (commit additional synchronous units) and/or dispatch down the binding contingency, depending on which decision is least-cost. Based on [23], it is taken here that $\left|\overline{ROCOF}\right| = 0.5$ Hz/s.

Due to inherent delays in the response—as a result of measurement delays, the presence of an activation deadband, and an initial response time constant (so as to guard against detrimental drive train stresses that can arise from high rates of change of power output)—commercial wind power emulated inertia schemes are considered here to not impact upon the initial system RoCoF of low inertia power systems [46]. Hence, only synchronous resources are considered for (15) and (17).

III. RoCoF Impacts of Non-Synchronous Reserve Resources

For each case under each scenario (see Section II-G), hourly resolution UCED schedules are determined for one year of operation. Following completion of a full UCED simulation, the time periods are used to initialise frequency stability time domain simulation, for the loss of the largest infeed during those time periods. Equation (13) is applied to the results of each time domain simulation, and the resulting RoCoF magnitude statistics are detailed in Fig. 5, which shows the mean and maximum values. In both the current and future operational scenarios, the mean system RoCoF is ∼5.7% higher in the sync+non-sync case in comparison to that in the sync-only case. For both cases under the future operational scenario, the maximum post-event RoCoF magnitude is kept below $\left|\overline{ROCOF}\right|$, due to (17) being employed. In contrast, under the current operational scenario, with (15) employed, there is a higher maximum RoCoF magnitude, particularly in the sync+non-sync case.

In order to explore the changes in pre-contingency operating conditions which result in the degradation of system RoCoF performance, Fig. 6 shows, for each operational scenario, the difference in post-contingency RoCoF magnitude between

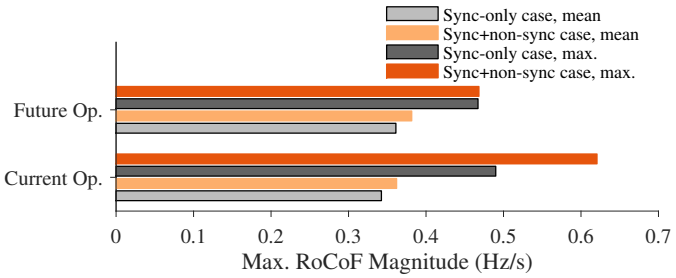

Fig. 5. Mean and maximum of the $|rocof^{max}|$ dataset for the sync-only and sync+non-sync cases under the current and future operational scenarios

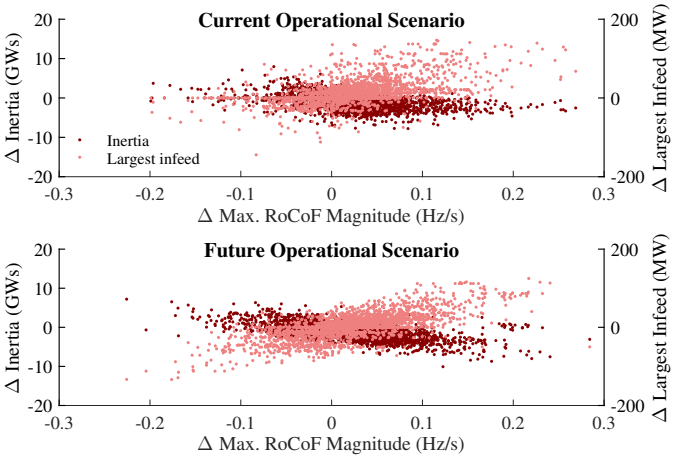

Fig. 6. Impact of changes in inertia and largest infeed online, between the sync-only and sync+non-sync cases, on post-event maximum RoCoF magnitude (Δ = sync+non-sync case value − sync-only case value)

the sync-only and sync+non-sync cases as a function of the change in the largest infeed and the system inertia level, for each time period. Fig. 6 demonstrates that there is a general trend of both lower system inertia and larger active power infeeds with non-synchronous reserve provision—trends that, as shown in Fig. 5, have a detrimental impact on the system RoCoF performance.

In order to reveal the causes of increased largest infeeds, Fig. 7 shows the change in the number of hours that conventional generators, categorised per fuel type, spend at maximum capacity, between the sync-only and sync+non-sync cases. In the presence of a non-synchronous reserve resource, the greatest increase is seen for CCGTs and coal-fired thermal units, as the need for contingency reserve from such low marginal cost units decreases significantly.

In systems with nuclear units, or any other large, inflexible base load, an increase in largest infeed magnitude is less likely, given that nuclear units already spend considerable time near maximum power output when online. However, in such systems there would likely be an increase in the output of other online units, increasing the likelihood of higher RoCoF magnitudes following their loss, or for N−1−1 events.

The number of 'inertia-heavy' (>1 GWs) synchronous generators online, ranked to form duration curves, is shown in Fig. 8. With non-synchronous reserve in sufficient volumes, times during which generation was committed for reserve

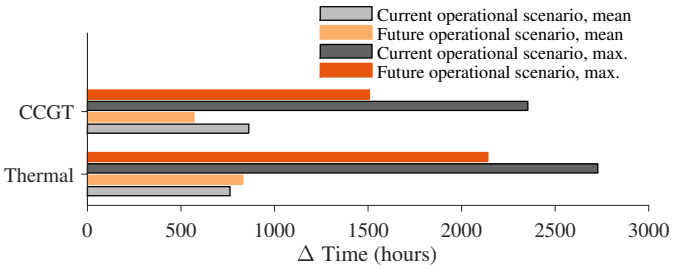

Fig. 7. Mean and maximum change in time spent at maximum output, per fuel type, between the sync-only and sync+non-sync cases (Δ = sync+non-sync case value − sync-only case value)

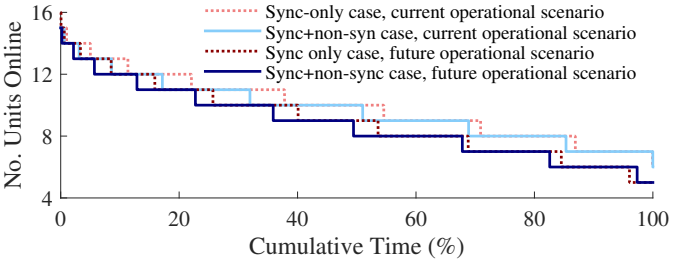

Fig. 8. Number of inertia-heavy generating units online

purposes are now significantly reduced, yielding a reduction in the number of synchronous units online in the sync+non-sync cases. Note that, for a given operational scenario, the minimum number of conventional units online does not decrease between the sync-only and sync+non-sync cases. Such a trend is due to the availability of EWH: the periods of high-low EWH availability coincide with the nascent high-low (day-night) system inertia level: if the converse were true, the minimum number of conventional generators would likely decrease due to the presence of non-synchronous reserve resources (as can occur with wind power).

IV. Incorporation of Non-Synchronous Reserve Resources

Any operational policy change must include the weighing of efficiency gains, trade-offs, and system operational security impacts. A matrix of criteria for which system operators could assess the impact of the integration of non-synchronous reserve resources is presented in Table IV. Here, scheduling indices, namely: production cost, CO_2 emission, ramping burden (the product of the time spent ramping and the ramp magnitudes), and variable RES (in this case, wind) curtailment, are compared alongside short-term frequency stability indices, namely: nadir, steady-state post-event deviation, maximum rate of change, and number of times that static responses are triggered.

A. Scheduling Metrics

The inclusion of non-synchronous reserve resources (assumed here to have low-cost bids) tends to reduce the production cost. The coincidence between time periods of high non-synchronous reserve availability and high contingency reserve requirement is an important characteristic that drives

TABLE IV
EVALUATION MATRIX (YEAR-LONG SIMULATIONS)

		Scheduling Metrics				*Frequency Stability Metrics*			
Operational Scenario	Reserve Case	Production Cost (M€)	CO_2 Production (Mtonne)	Variable RES Curtailment (%)	Ramping Burden (TWh)	Mean Steady-State Deviation (Hz)	Mean Nadir (Hz)	Simulations with Static Responses Used (%)	Mean RoCoF (Hz/s)
Current	Sync-only	11,826	13.76	3.50	13.39	0.21	49.57	56.51	**0.34**
	Sync+non-sync	**11,803**	**13.61**	**3.21**	**11.41**	**0.20**	**49.67**	**19.66**	0.36
Future	Sync-only	11,589	**12.24**	5.00	14.26	0.19	49.56	63.29	**0.36**
	Sync+non-sync	**11,533**	12.31	**4.10**	**12.08**	0.19	**49.66**	**25.27**	0.38

production cost savings. The variability of non-synchronous reserve availability is also of note. Taking EWH as an example, a higher upward/downward contingency reserve availability is dependent on the number of appliances being in the on/off state, the probability of which is a function of the time of day, week and season. Considering a number of flexible loads in concert [47], if chosen appropriately, can smooth variability, potentially resulting in higher volumes of loads being scheduled for contingency reserve provision. If there is high temporal variability of non-synchronous reserve availability, such reserve resources are likely to have low utilisation—even if there is high availability during particular time periods—due to the temporal constraints of the conventional units that are required to provide reserve in adjacent time periods.

In relation to CO_2 production, non-synchronous reserve resources have a contrasting effect in each operational scenario. In the current operational scenario, (15) is in place, which tends to commit additional CCGTs (at part-load), given their high inertia. The presence of non-synchronous reserve resources increases the utilisation factor (and hence fossil-fuel-burn efficiency) of CCGTs, resulting in lower CO_2 production in the sync+non-sync case. For the future operational scenario, (17) is in place, which, as opposed to committing high-inertia units, tends to opt for a dispatch-down decision when the binding contingency is a generator. As a consequence, CCGT capacity factors are reduced (in comparison with an inertial floor being in place), resulting in higher coal unit capacity factors. The presence of non-synchronous reserve resources increases coal outputs further (no longer part-loaded for reserve provision), which increases the total CO_2 production. Thus, the potential benefits of non-synchronous reserve resources may not be fully realized if coupled with base-load coal. However, it must be noted that if (15) were employed in the future operational scenario higher CO_2 production and variable RES curtailment arises, in comparison to employing (17).

Regarding variable RES curtailment, the lower number of conventional units online in the sync+non-sync cases yields a reduction under both operational scenarios. Due to downward flexibility reserve requirements, some conventional units are not permitted to be dispatched down to minimum output, which can result in wind curtailment at night. Such instances could be reduced if other reserve resources were included in the downward flexibility reserve constraint.

B. Frequency Stability Metrics

With time constants typically less than those associated with the control of hydraulic, steam or gas turbines, faster response times can be expected from non-synchronous resources in comparison to conventional generation governor response [48]. Thus, the magnitude of system frequency deviations can be reduced, as shown here (Table IV), and by others, such as [49]. The extent of the frequency deviation improvements gained by the integration of non-synchronous resources is a function of their frequency control capability. Here, EWH is the sole non-synchronous resource employed for frequency support, with a response time of 300 ms selected. In reality, subject to the physical properties of a given resource, there will be a range of frequency control techniques and parameters employed by non-synchronous resources to meet frequency response grid code/system service definitions. However, faster responses, such as that shown here for EWH, will tend to be favoured (see Fig. 1). Note that a 'fast as possible' response is not necessarily desirable from non-synchronous resources: care is needed to ensure that 'hunting' does not occur between fast frequency response providers and (slower) primary frequency response providers.

While it is shown that the magnitude of system frequency deviations can be reduced with the introduction of non-synchronous reserve, note that an explicit maximum frequency deviation constraint, as proposed in [16], [17], [50], is not included within the UCED model. The frequency deviation is implicitly accounted for through the primary operating reserve category, see (2) and (3).

With additional numbers of frequency governing resources online, here due to the aggregation of distributed load resources, the mean quasi-steady-state frequency deviation can be improved. Such a benefit is somewhat offset by the reduced utilisation of the static responses, which tend to improve the steady-state frequency deviation when triggered.

With respect to RoCoF, a slight worsening of the system performance may not be an urgent concern for systems with low non-synchronous shares, or for systems with a high level of high-inertia low-marginal-cost generators, e.g. a system with a large nuclear fleet. Some systems may also have loads that are not directly metered by the system operator, e.g. industrial load that is netted with internal/behind-the-meter generators. Such generation may be an important residual store of inertia. However, during periods of low market prices, e.g.

high wind power outputs at night, residual inertial stores may reduce as behind-the-meter industrial loads source power from the grid as opposed to from on-site sources.

V. Concluding Remarks

The scheduling of reserve from non-synchronous resources such as demand response, battery energy storage, wind power and solar photovoltaics is expected to increase significantly in the future.

It is shown here that the provision of reserve from a non-synchronous resource has two distinct effects on the synchronous generation fleet. Firstly, there is an increase in the active power outputs of low marginal cost units, as they are less often needed to be part-loaded for reserve provision. Secondly, higher marginal cost units that were previously online for reserve provision are more commonly de-committed. The latter effect is similar to that experienced for energy provision from non-synchronous resources: the underlying cause of system inertial reduction arises from a given resource's low marginal cost and non-synchronous nature. The former effect exacerbates the worsening of RoCoF performance in a low inertia scenario, due to the increased generator outputs for N$-$1 events online.

In order to address the resulting degradation in system RoCoF, a commitment-and-dispatch RoCoF constraint within UCED has been proposed, which explicitly considers the commitment status and active power output of synchronous resources, as well as the N$-$1 contingency set. Such a formulation allows for commitment and/or dispatch decisions to be made in order to efficiently satisfy RoCoF requirements, if binding. Though perfect foresight of wind power is assumed, the RoCoF formulation presented is generalised, and thus easily adapted for incorporating uncertainty within UCED.

As well as the formulation itself, e.g. inertia floor versus commitment-and-dispatch RoCoF, the operational impacts of a constraint, e.g. cost and variable RES curtailment, are a function of the specified requirement. In order to further increase operational efficiency, measures should be pursued that allow for constraint relaxation or for the requirement to be met more efficiently. An example of the former approach could be procuring reserve products with a faster speed of response, while the latter approach could involve incentivising synchronous inertia to be committed on a more flexible/granular basis, e.g. synchronous condensers, lower generator minimum loads, multi-mode operation.

Here, one candidate non-synchronous reserve resource, namely demand response from EWH, is modelled. In reality, of course, there will be diversity in the non-synchronous reserve resource fleet, with the effect of a particular non-synchronous resource type on the probabilistic distribution of system RoCoF dependent on its aggregate availability, e.g. correlations with patterns of net load, system inertia and largest online contingencies.

Other potential metrics to incorporate within the evaluation matrix include the following. (i) Forecast errors of a given non-synchronous reserve resource. If increasing levels of reserve is provided by non-conventional resources, certainty of reserve availability will become increasingly important. System operators may stipulate that each resource should indicate its forecasted availability to provide reserve over a given time horizon, with an incentive linked to the accuracy of the declared forecast. For example, the uncertainty associated with the provision of wind power emulated inertial response (which requires knowledge of the number of capable wind turbines online) is likely higher than that associated with provision from battery energy storage. More generally, representing the forecast error of RES within UCED is increasing in importance, with a range of implementations proposed [51]. (ii) If contingency reserve is sourced from synchronously-connected rotating loads, the (further) reduction in system inertia following the activation of a response.

Acknowledgment

The primary author would like to dearly thank J. Ryan (An Mhí) for his generous modelling advise.

References

[1] K. Das, M. Altin, A. D. Hansen, P. E. Sørensen, and H. Abildgaard, "Primary reserve studies for high wind power penetrated systems," in *IEEE PES PowerTech*, Eindhoven, The Netherlands, 2015.

[2] GE Energy Consulting, "Technology Capabilities for Fast Frequency Response," AEMO, Mar. 2017.

[3] National Grid, "Testing Guidance for Providers of Enhanced Frequency Response Balancing Service," Mar. 2017.

[4] EirGrid and SONI, "DS3 System Services Scalar Design Recommendations Paper," Oct. 2017.

[5] P. Daly, N. Cunniffe, and D. Flynn, "Inertia considerations within unit commitment and economic dispatch for systems with high non-synchronous penetrations," in *IEEE PES PowerTech*, Eindhoven, The Netherlands, 2015.

[6] L. Meegahapola and D. Flynn, "Characterization of gas turbine lean blowout during frequency excursions in power networks," *IEEE Trans. Power Syst.*, vol. 30, no. 4, pp. 1877–1887, July 2015.

[7] D. Reimert, *Protective Relaying for Power Generation Systems*. CRC Press, 2006.

[8] W. Freitas, W. Xu, C. M. Affonso, and Z. Huang, "Comparative analysis between ROCOF and vector surge relays for distributed generation applications," *IEEE Trans. Power Del.*, vol. 20, no. 2, pp. 1315–1324, Apr. 2005.

[9] F. A. M. Moura, J. R. Camacho, G. C. Guimaraes, and M. L. R. Chaves, "Steam turbines under abnormal frequency conditions in distributed generation systems," in *Mechanical Engineering*. InTech, 2012.

[10] S. Barnes *et al.*, "High fidelity approach to analysing combined-cycle power plant response to proposed ROCOF requirements in Ireland," in *CIGRÉ Session 46*, Paris, France, 2016.

[11] DNV KEMA, "An Independent Analysis on the Ability of Generators to Ride Through Rate of Change of Frequency values up to 2 Hz/s," EirGrid and SONI, Feb. 2013.

[12] M. Aunedi, P. A. Kountouriotis, J. E. O. Calderon, D. Angeli, and G. Strbac, "Economic and environmental benefits of dynamic demand in providing frequency regulation," *IEEE Trans. Smart Grid*, vol. 4, no. 4, pp. 2036–2048, Dec. 2013.

[13] Y. Wen, C. Y. Chung, and X. Ye, "Enhancing frequency stability of asynchronous grids interconnected with HVDC links," *IEEE Trans. Power Syst.*, vol. 33, no. 2, pp. 1800–1810, Mar. 2018.

[14] Y. Wen, W. Li, G. Huang, and X. Liu, "Frequency dynamics constrained unit commitment with battery energy storage," *IEEE Trans. Power Syst.*, vol. 31, no. 6, pp. 5115–5125, Nov. 2016.

[15] E. Ela, V. Gevorgian, A. Tuohy, B. Kirby, M. Milligan, and M. O'Malley, "Market designs for the primary frequency response ancillary service—part I: motivation and design," *IEEE Trans. Power Syst.*, vol. 29, no. 1, pp. 421–431, Jan. 2014.

[16] F. Teng, V. Trovato, and G. Strbac, "Stochastic scheduling with inertia-dependent fast frequency response requirements," *IEEE Trans. Power Syst.*, vol. 31, no. 2, pp. 1557–1566, Mar. 2016.

[17] H. Ahmadi and H. Ghasemi, "Security-constrained unit commitment with linearized system frequency limit constraints," *IEEE Trans. Power Syst.*, vol. 29, no. 4, pp. 1536–1545, July 2014.

[18] J. F. Restrepo and F. D. Galiana, "Unit commitment with primary frequency regulation constraints," *IEEE Trans. Power Syst.*, vol. 20, no. 4, pp. 1836–1842, Nov. 2005.

[19] R. Doherty, G. Lalor, and M. O'Malley, "Frequency control in competitive electricity market dispatch," *IEEE Trans. Power Syst.*, vol. 20, no. 3, pp. 1588–1596, 2005.

[20] CRU and UREG, "Validated SEM PLEXOS Forecast Model for 2012–13," 2012.

[21] IEA, "World Energy Outlook 2013," Nov. 2013.

[22] National Grid, "Electricity Ten Year Statement," Nov. 2012.

[23] EirGrid and SONI, "Operational Constraints Update 13/07/2017," Accessed on: Aug. 15, 2017. [Online]. Available: http://www.eirgridgroup.com/site-files/library/EirGrid/Operational-Constraints-Update-July-2017.pdf

[24] ——, "All-Island Ten Year Transmission Forecast Statement 2016," 2017.

[25] Energy Exemplar, "PLEXOS Simulation Software," Accessed on: June 5, 2015. [Online]. Available: https://energyexemplar.com/products/plexos-simulation-software/

[26] FICO, "Xpress Solver," Accessed on: June 5, 2015. [Online]. Available: http://www.fico.com/en/products/fico-xpress-solver/

[27] EirGrid and SONI, "Clarification Note on Dynamic versus Static Response," May 2016.

[28] J. O'Sullivan *et al.*, "Studying the maximum instantaneous non-synchronous generation in an island system—frequency stability challenges in Ireland," *IEEE Trans. Power Syst.*, vol. 29, no. 6, pp. 2943–2951, Nov. 2014.

[29] EirGrid and SONI, "DS3 Programme Operational Capability Outlook 2016," May 2016.

[30] O. Ma *et al.*, "Demand response for ancillary services," *IEEE Trans. Smart Grid*, vol. 4, no. 4, pp. 1988–1995, Dec. 2013.

[31] A. Abiri-Jahromi and F. Bouffard, "Contingency-type reserve leveraged through aggregated thermostatically-controlled loads—part II: case studies," *IEEE Trans. Power Syst.*, vol. 31, no. 3, pp. 1981–1989, May 2016.

[32] U. Jordan and K. Vajen, "Realistic Domestic Hot-Water Profiles in Different Time Scales," IEA-SHC Task 26, May 2001.

[33] J. Kondoh, N. Lu, and D. J. Hammerstrom, "An evaluation of the water heater load potential for providing regulation service," *IEEE Trans. Power Syst.*, vol. 26, no. 3, pp. 1309–1316, Aug. 2011.

[34] S. A. Pourmousavi, S. N. Patrick, and M. H. Nehrir, "Real-time demand response through aggregate electric water heaters for load shifting and balancing wind generation," *IEEE Trans. Smart Grid*, vol. 5, no. 2, pp. 769–778, Mar. 2014.

[35] MathWorks, "MATLAB & Simulink," Accessed on: Nov. 16, 2015. [Online]. Available: https://uk.mathworks.com

[36] F. P. deMello *et al.*, "Dynamic models for fossil fueled steam units in power system studies," *IEEE Trans. Power Syst.*, vol. 6, no. 2, pp. 753–761, May 1991.

[37] G. Lalor, J. Ritchie, D. Flynn, and M. O'Malley, "The impact of combined-cycle gas turbine short-term dynamics on frequency control," *IEEE Trans. Power Syst.*, vol. 20, no. 3, pp. 1456–1464, Aug. 2005.

[38] F. P. deMello *et al.*, "Hydraulic turbine and turbine control models for system dynamic studies," *IEEE Trans. Power Syst.*, vol. 7, no. 1, pp. 167–179, Feb. 1992.

[39] K. Clark, N. W. Miller, and J. J. Sanchez-Gasca, "Modeling of GE Wind Turbine-Generators for Grid Studies Version 4.5," Apr. 2010.

[40] J. W. O'Sullivan and M. J. O'Malley, "Identification and validation of dynamic global load model parameters for use in power system frequency simulations," *IEEE Trans. Power Syst.*, vol. 11, no. 2, pp. 851–857, May 1996.

[41] EirGrid, "Grid Code Modification Proposal (MPID 229): Rate of Change of Frequency," Sept. 2012.

[42] P. J. Douglass, R. Garcia-Valle, P. Nyeng, J. Østergaard, and M. Togeby, "Smart demand for frequency regulation: experimental results," *IEEE Trans. Smart Grid*, vol. 4, no. 3, pp. 1713–1720, Sept. 2013.

[43] V. Trovato, I. Martínez Sanz, B. Chaudhuri, and G. Strbac, "Advanced control of thermostatic loads for rapid frequency response in Great Britain," *IEEE Trans. Power Syst.*, vol. 32, no. 3, pp. 2106–2117, May 2017.

[44] Y.-Q. Bao and Y. Li, "FPGA-based design of grid friendly appliance controller," *IEEE Trans. Smart Grid*, vol. 5, no. 2, pp. 924–931, Mar. 2014.

[45] J. Lian, Y. Sun, L. D. Marinovici, and K. Kalsi, "Improved controller design of Grid Friendly™ appliances for primary frequency response," in *IEEE PES General Meeting*, Denver, CO, USA, 2015.

[46] L. Ruttledge, N. W. Miller, J. O'Sullivan, and D. Flynn, "Frequency response of power systems with variable speed wind turbines," *IEEE Trans. Sustain. Energy*, vol. 3, no. 4, pp. 683–691, Oct. 2012.

[47] H. W. Qazi and D. Flynn, "Synergetic frequency response from multiple flexible loads," *Electr. Power Syst. Res.*, vol. 145, pp. 185–196, 2017.

[48] M. Cheng *et al.*, "Power system frequency response from the control of bitumen tanks," *IEEE Trans. Power Syst.*, vol. 31, no. 3, pp. 1769–1778, May 2016.

[49] J. A. Short, D. G. Infield, and L. L. Freris, "Stabilization of grid frequency through dynamic demand control," *IEEE Trans. Power Syst.*, vol. 22, no. 3, pp. 1284–1293, Aug. 2007.

[50] H. Chavez, R. Baldick, and S. Sharma, "Governor rate-constrained OPF for primary frequency control adequacy," *IEEE Trans. Power Syst.*, vol. 29, no. 3, pp. 1473–1480, May 2014.

[51] K. Bruninx and E. Delarue, "Endogenous probabilistic reserve sizing and allocation in unit commitment models: cost-effective, reliable, and fast," *IEEE Trans. Power Syst.*, vol. 32, no. 4, pp. 2593–2603, July 2017.

Pádraig Daly received the Ph.D. degree from the University College Dublin, Dublin, Ireland, in 2018. He is currently working in industry. His research interests include power system operations, planning, and decarbonisation.

Hassan W. Qazi received the Ph.D. degree from the University College Dublin, Dublin, Ireland, in 2015. His research interests include renewable integration, advanced modelling and demand response.

Damian Flynn (M'96–SM'11) is an Associate Professor of power system operation and control with the University College Dublin, Dublin, Ireland. His research interests include power system analysis and control, and the integration of renewable generation in to electrical networks, and advanced modeling and control techniques applied to power plant. He is an Editor for the IEEE TRANSACTIONS ON ENERGY CONVERSION.